Electronic Supporting Information

High activity nano-structured vanadium-nitrogen supported nickel foam as electrode for efficient electrocatalytic oxidation of benzyl alcohol

Handan Chen, Zhifei Zhu, Yizhen Zhu, Mei Kuai, Kejie Chai,* and Weiming Xu*

College of Material, Chemistry and Chemical Engineering, Hangzhou Normal University, Hangzhou 311121, China.

E-mail: wmxu@zju.edu.cn (W.M. Xu)

E-mail: kjchai@foxmail.com (K.J. Chai)

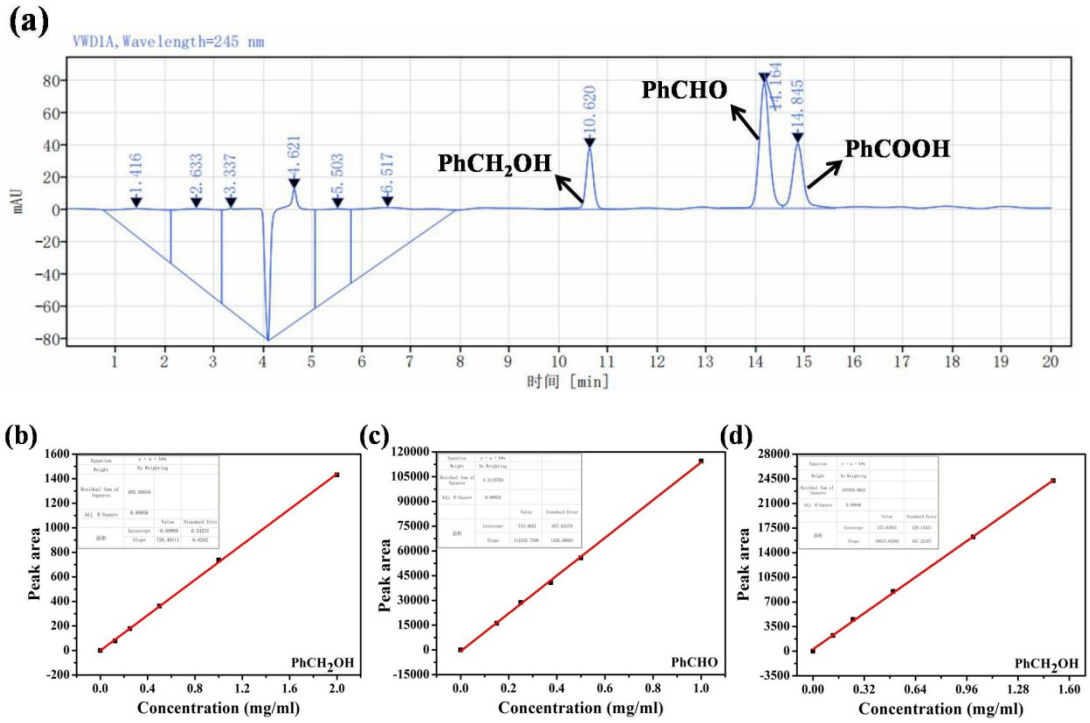

Figure S1. (a) The peak time of the benzyl alcohol, benzaldehyde and benzoic acid; Standard curves: (b) benzyl alcohol, (c) benzaldehyde, (d) benzoic acid.

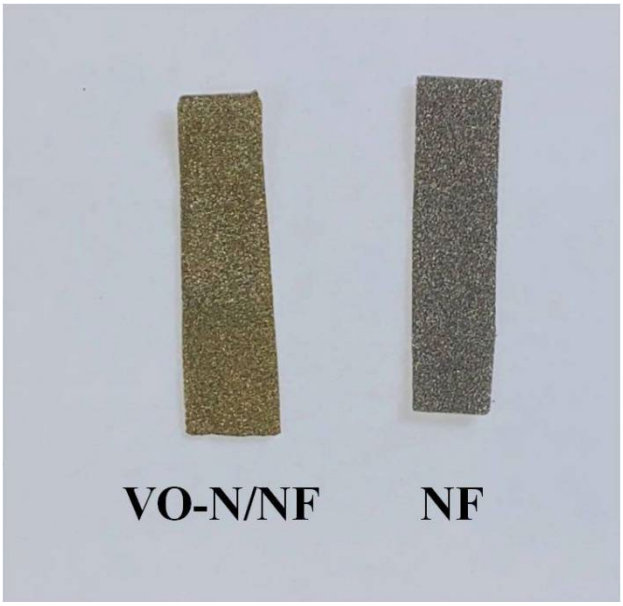

Figure S2. Picture of the VO-N/NF nanocomposite before and after the hydrothermal reaction.

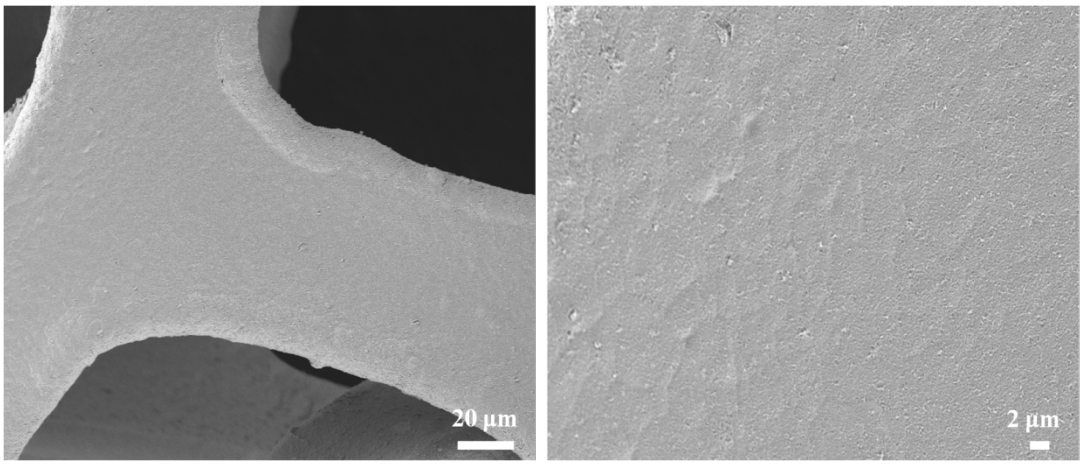

Figure S3. SEM image of the bare nickel foam.

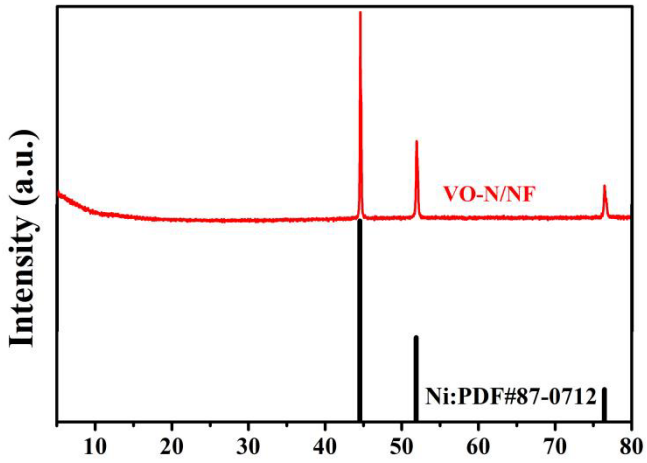

Figure S4. XRD pattern of the VO-N/NF nanocomposite.

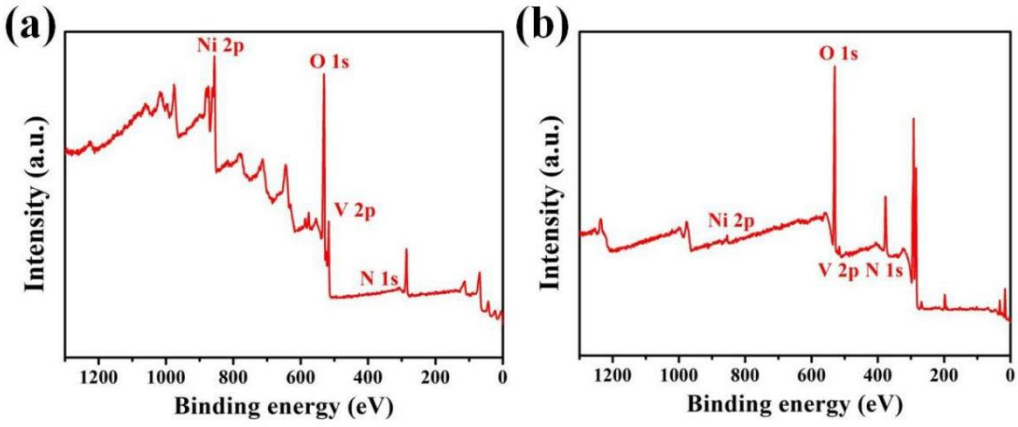

Figure S5. XPS spectra of the VO-N/NF nanocomposite (a) before and (b) after multiple reactions.

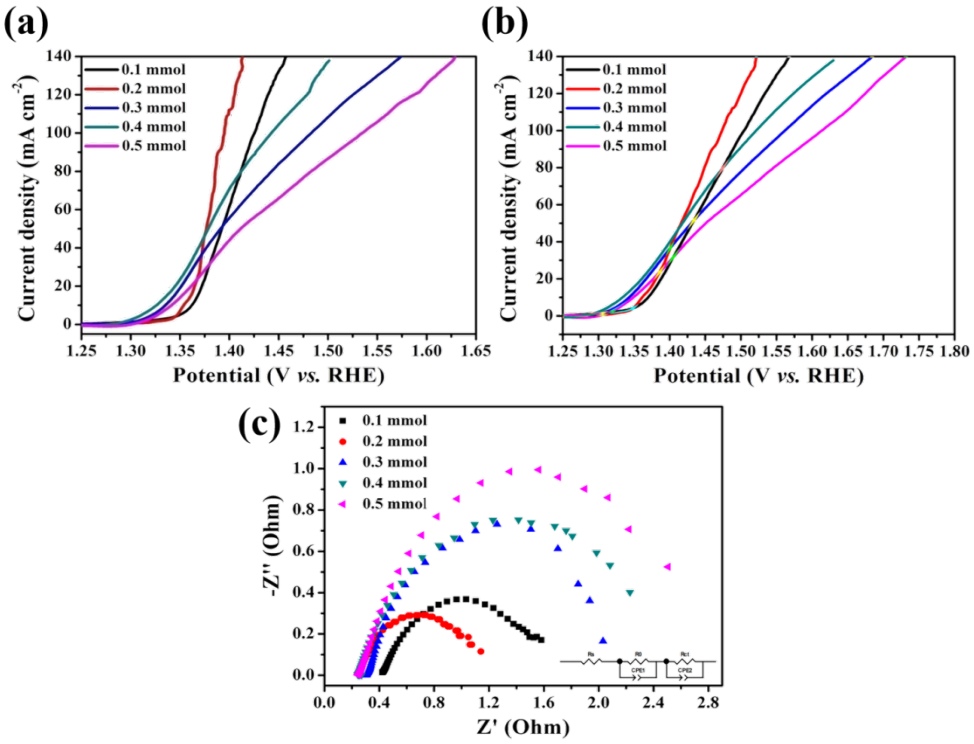

Figure S6. LSV plots for VO-N/NF nanocomposite with different concentrations of precursors (a) under IR correction and (b) without IR correction,(c) EIS spectra for VO-N/NF nanocomposite with different concentrations of precursors

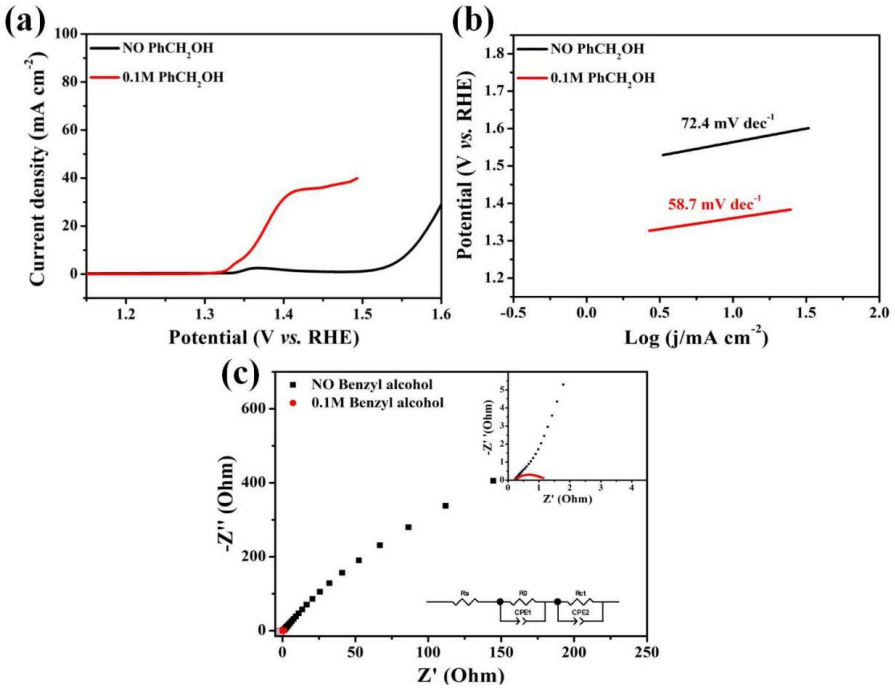

Figure S7. (a) LSV plots of NF, (b) Tafel scope of NF and (c) EIS spectra of VO-N/NF nanocomposite for benzyl alcohol oxidation and OER.

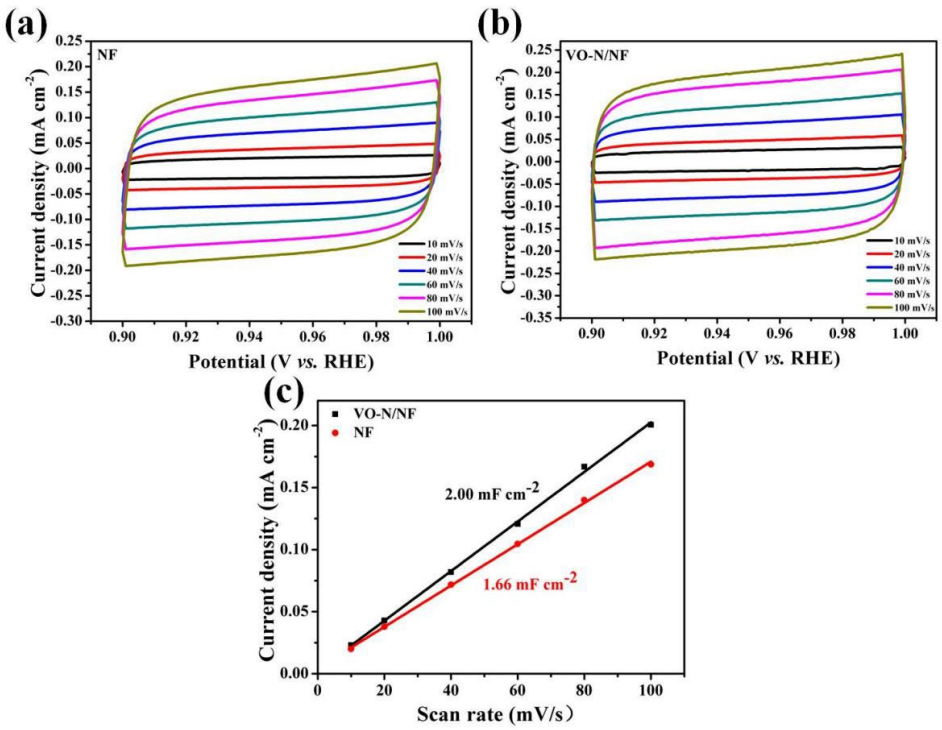

Figure S8. The CV diagram of (a) NF, (b) VO-N/NF nanocomposite and (c) C_{dl} plot of VO-N/NF nanocomposite and NF in 1.0 M KOH with 0.1 M benzyl alcohol.

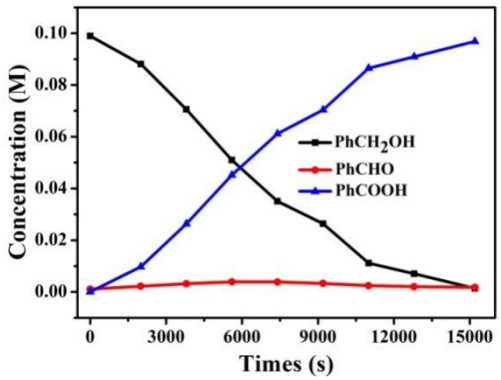

Figure S9. Concentration of each product during the process of electrocatalytic benzyl alcohol oxidation with NF.

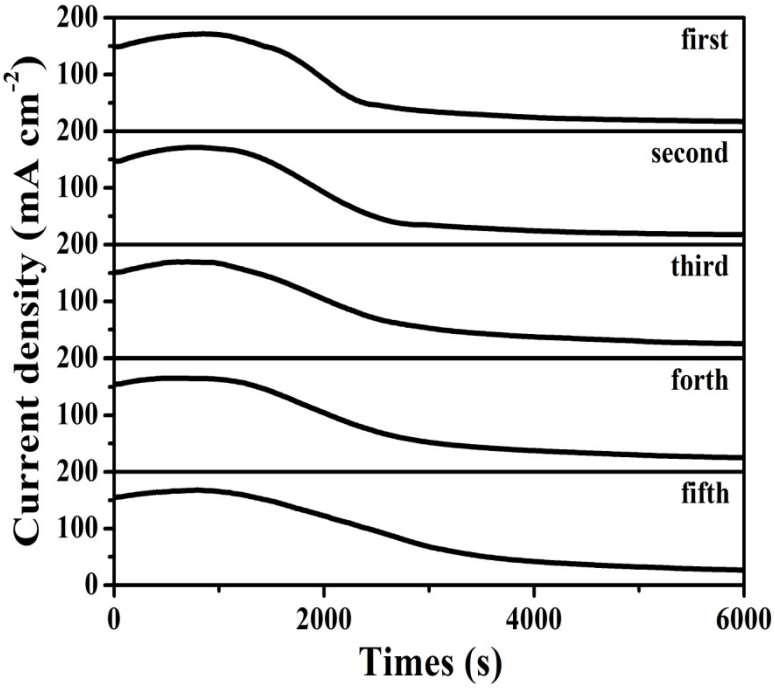

Figure S10. Chronoamperometry tests of electrocatalytic benzyl alcohol oxidation for five cycles.

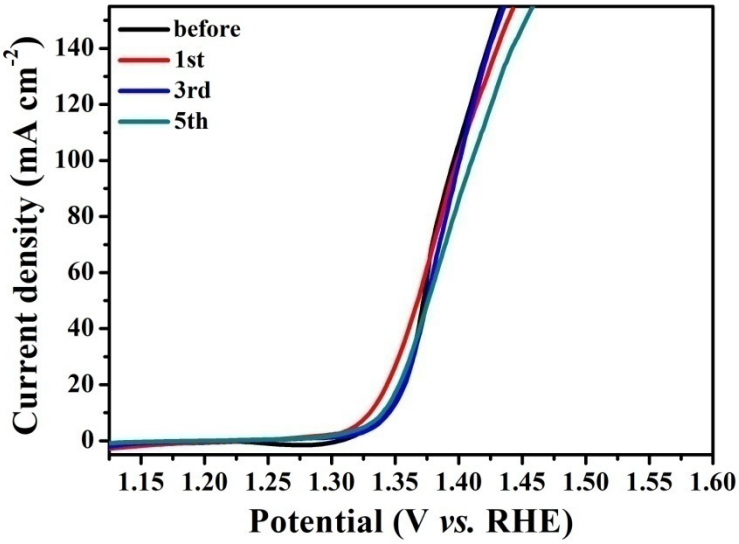

Figure S11. The LSV plots of VO-N/NF nanocomposite under IR correction.

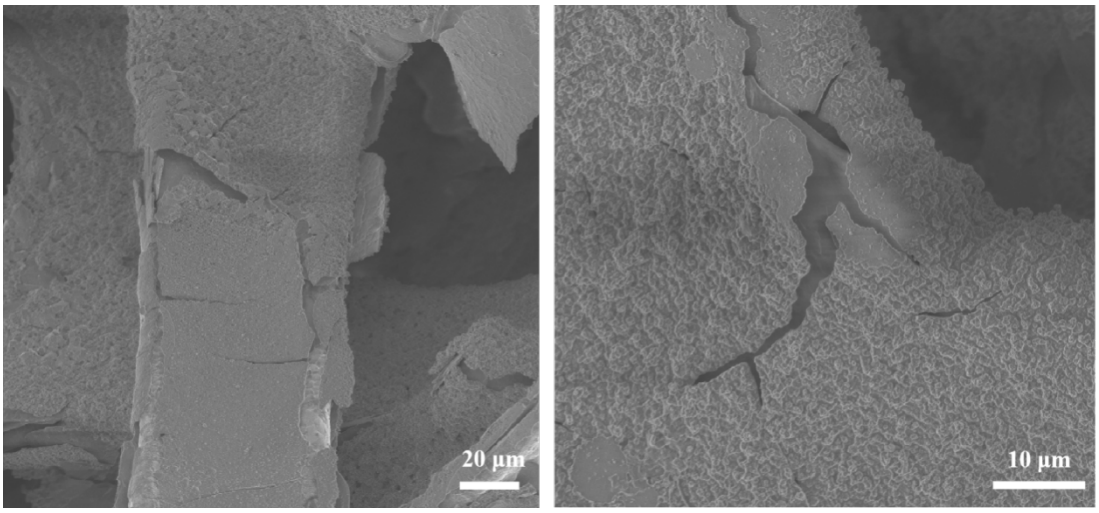

Figure S12. SEM image of VO-N/NF nanocomposite after electrocatalytic oxidation of benzyl alcohol.

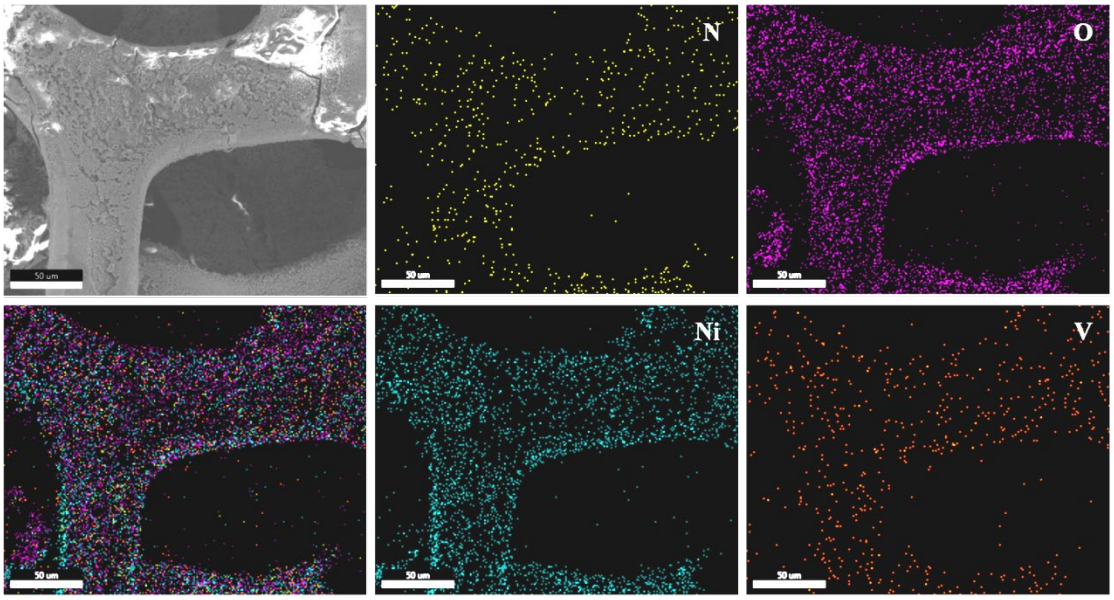

Figure S13. EDS mapping image of VO-N/NF after electrocatalytic oxidation of benzyl alcohol.

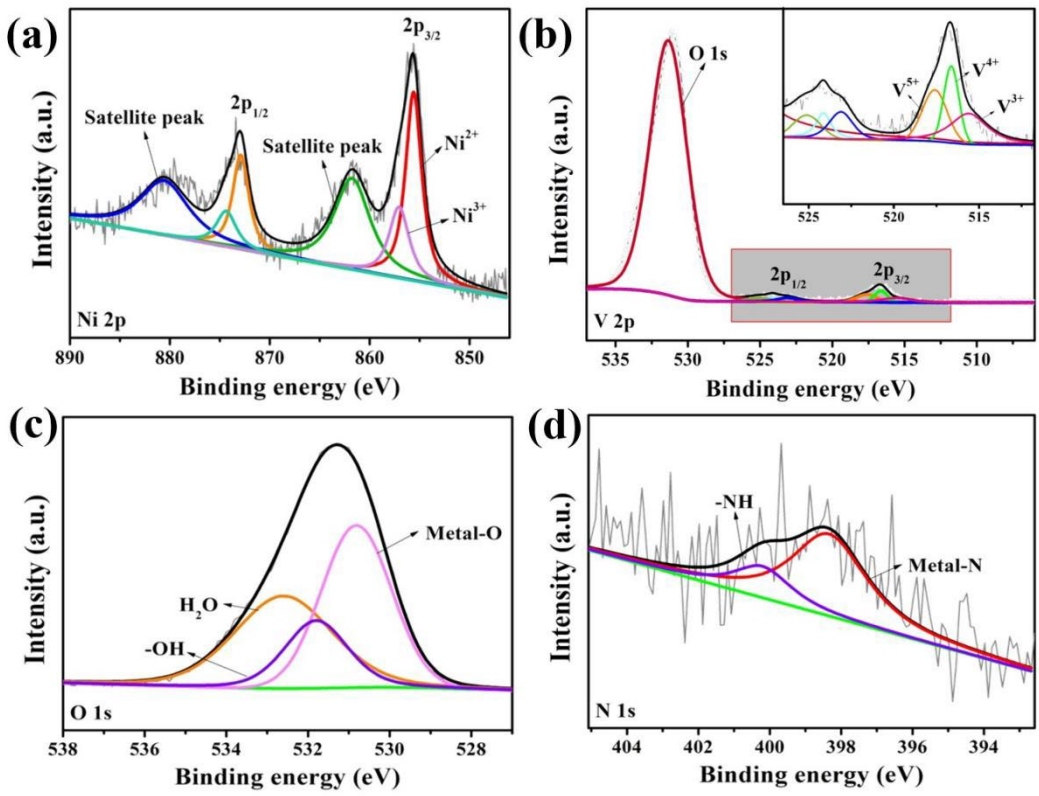

Figure S14. XPS spectrums of (a) Ni 2p, (b) V 2p, (c) O 1s and (d) N 1s for VO-N/NF nanocomposite after five cycles.

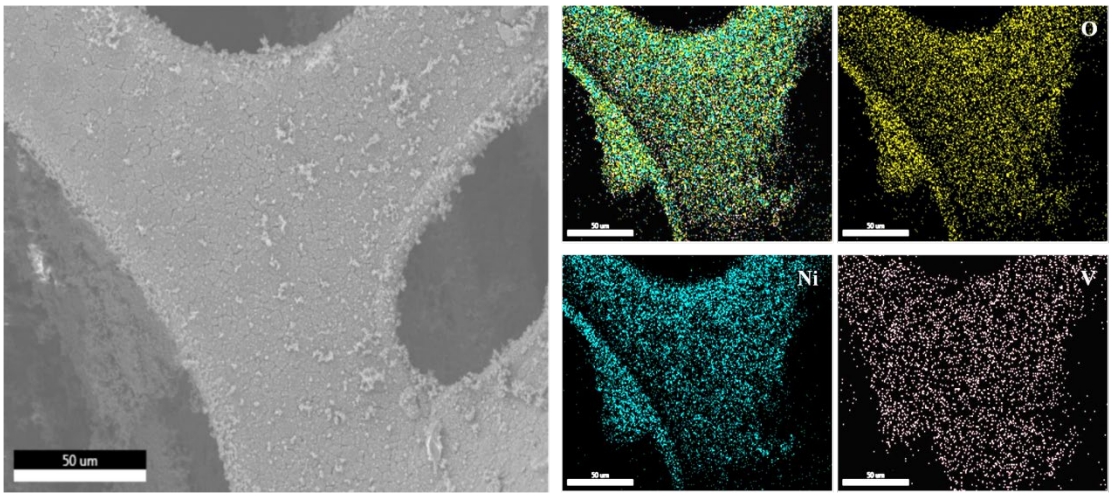

Figure S15. EDS mapping image of VO/NF.

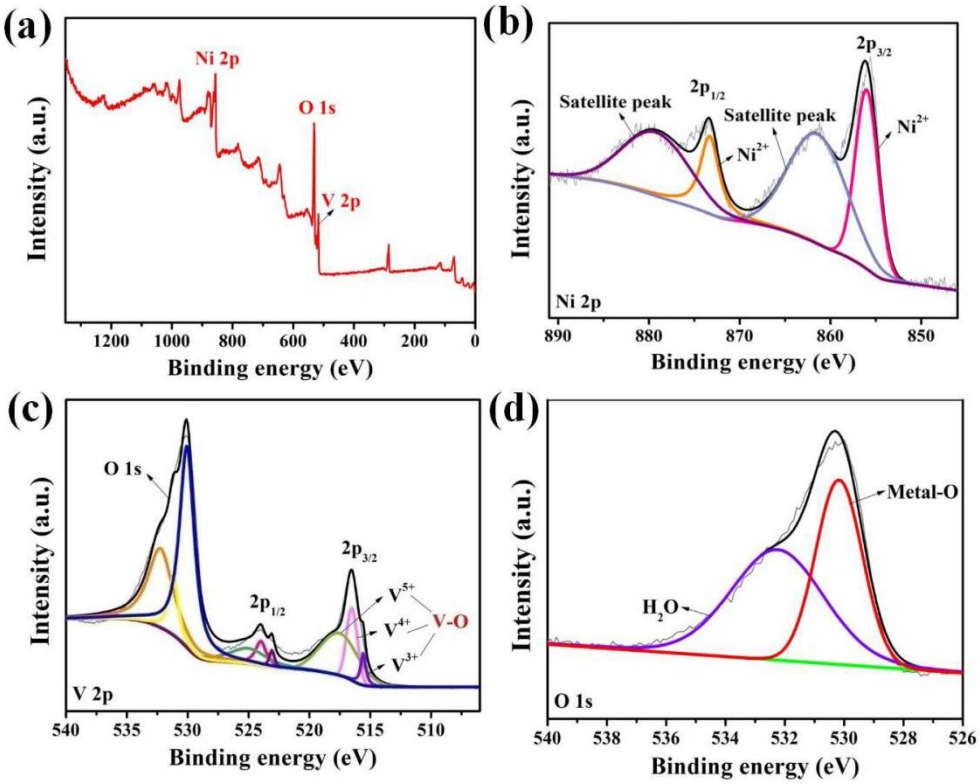

Figure S16. XPS spectrums of (a) whole pattern, (b) Ni 2p, (c) V 2p and (d) O 1s for VO/NF electrode.

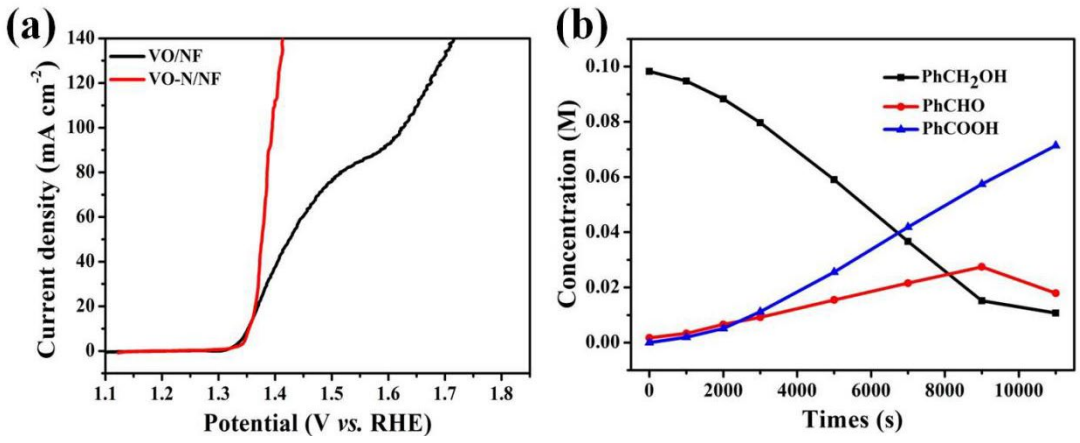

Figure S17. (a) The LSV plot of VO-N/NF nanocomposite and VO/NF; (b) Concentration of each product during the process of electrocatalytic benzyl alcohol oxidation with VO/NF.

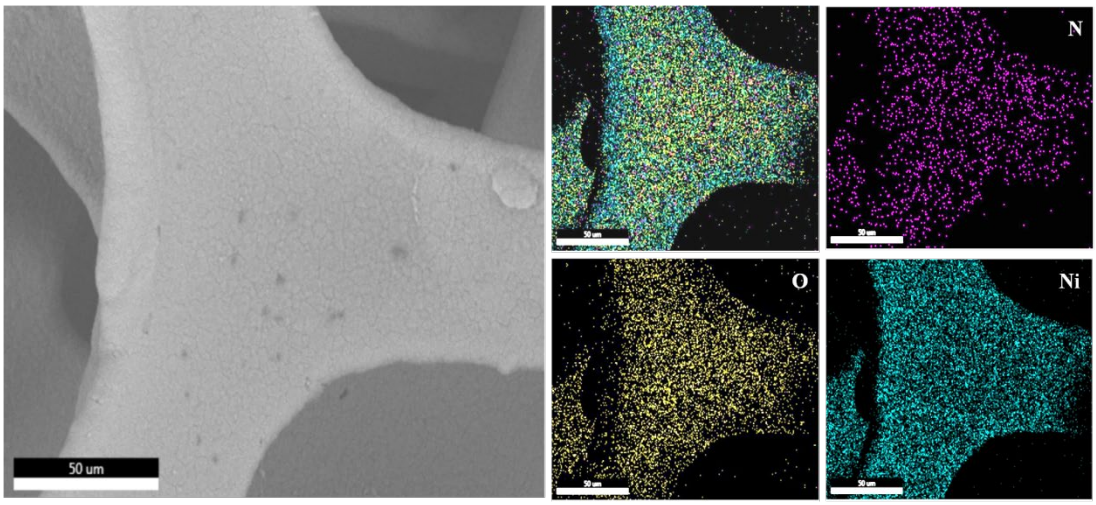

Figure S18. EDS mapping image of N/NF.

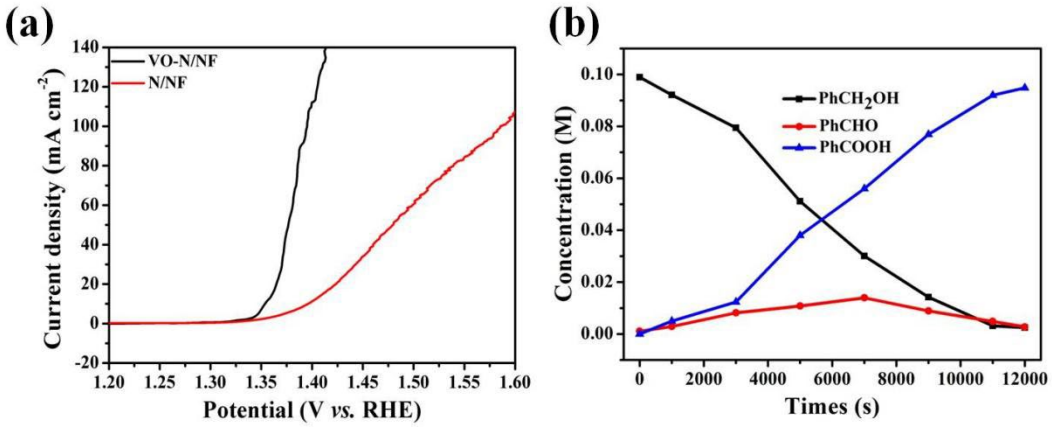

Figure S19. (a) The LSV plot of VO-N/NF nanocomposite and N/NF; (b) Concentration of each product during the process of electrocatalytic benzyl alcohol oxidation with N/NF.

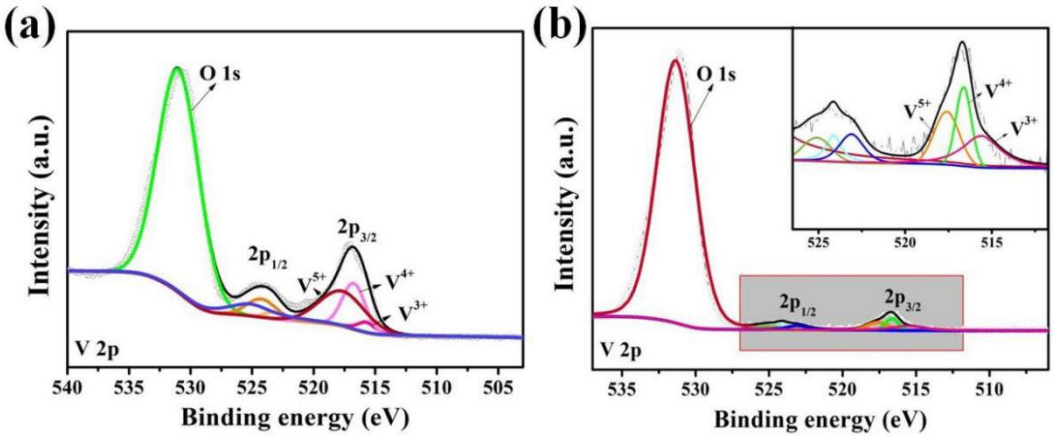

Figure S20. XPS spectrums of V 2p for VO-N/NF nanocomposite (a) before and (b) after five cycles.

Table S1. The percentage composition of N, V, O, and Ni elements in the VO-N/NF nanocomposite by EDS

Element	N	O	Ni	V
Proportion	8%	44%	42%	6%

Table S2. Impedance fitting results for VO-N/NF nanocomposite with different concentrations of precursors

Precursor content	0.1 mmol	0.2 mmol	0.3 mmol	0.4 mmol	0.5 mmol
Rct (Ω)	0.978	0.863	1.802	2.141	2.293

Table S3. The mass of V in per 100 mg VO-N/NF nanocomposite.

Precursor content	0.1 mmol	0.2 mmol	0.3 mmol	0.4 mmol	0.5 mmol
V/mg	0.73	1.19	1.26	1.87	2.26

Table S4. Impedance fitting results for VO-N/NF and NF electrodes.

	Rs (Ω)	R_{ct} (Ω)
VO-N/NF nanocomposite	0.244	0.863
NF	0.240	88.53

Table S5. Comparison of VO-N/NF nanocomposite electrodes with most existing electrodes in terms of precursor content and the performance of electrocatalytic benzyl alcohol oxidation.

Electrocatalyst	Electrolyte	Precursor content	Conv. (%)	FE (%)	Potential (*vs.* RHE) @Current density (mA cm^{-2})	Reference
VO-N/NF nanocomposite	1M KOH 0.1 M benzyl alcohol (BA)	0.2 mmol NH_4VO_3	99.7	99.3	1.395V@100	**This work**
Co_3O_4/NF	1 M KOH 0.020 M BA	0.8 mmol $Co(NO_3)_2{\cdot}6H_2O$ 0.008 mol $C_6H_{12}N_4$, 0.0072 mol $KBrO_3$ 0.0064 mol NH_4F	100	91.4	1.50V@86	[1]

Ni-OH/NF	1 M NaOH 0.1 M BA	0.1 M $Ni(NO_3)_2$	84.5	99	~1.33V@100	[2]
NC@$CuCoN_x$/CF	1 M KOH 0.015 M BA	0.5 mmol $Cu(NO_3)_2·3H_2O$ 1.0 mmol $Co(NO_3)_2·3H_2O$ 6 mmol urea	97.25	97.4	1.25V@10	[3]
A-Ni-Co-H/NF	1 M KOH 0.1 M BA	0.178 g urea 0.304 g $CoCl_2·6H_2O$	99.6	93.5	1.35V@100	[4]
N–Mo–Ni/NF	1 M KOH 0.1 M BA	0.06 mmol $(NH_4)_6Mo_7O_{24}·4H_2O$	99.1	98.7	1.395V@100	[5]
NiCo-61-MOF/NF	1 M NaOH 0.1 M BA	0.75 mol chloride salts 0.75 mol terephthalic acid	>86	-	1.25V@10	[6]
NiCo/AC	1 M KOH 0.1 M BA	0.09 g $Ni(NO_3)_2·6H_2O$ 0.45 g $Co(NO_3)_2·6H_2O$ 1.0 g activated carbon	-	-	1.425V@100	[7]
Ni@NC-280	1 M KOH 0.5 mmol BA	30 mg NC 6.6 mg $NiCl_2$	-	>99	1.39V@25	[8]
CC@NiO/Ni_3S_2	1 M KOH 0.2 M BA	0.5 g $NiCl_2·6H_2O$ 5.0 g CH_4N_2S	99.11	94.7	1.38V@10	[9]

Table S6. Comparison of VO-N/NF nanocomposite electrodes with most existing electrodes in terms of precursor content and the performance of other electrocatalytic oxidation.

Electrocatalyst	Electrolyte	Precursor content	Product	Potential (*vs.* RHE) @Current density (mA cm^{-2})	Reference
VO-N/NF nanocomposite	1 M KOH 0.1 M BA	0.2 mmol NH_4VO_3	PhCOOH	1.395V@100	**This work**
NiCo NMF	1 M KOH 1 M MeOH	0.1M $NiSO_4·6H_2O$ 0.1 M $CoSO_4·7H_2O$ 1 M $(NH_4)_2SO_4$	CH_2O HCOOK	1.33V@20	[10]

a-NiO_x/NF	1 M KOH 0.5 M urea	2 wt% Ni(II) 2-ethylhexanoate	N_2	~1.27V@100	[11]
O-NiMoP/NF	1 M KOH 0.5 M urea	0.2 M $NiSO_4·6H_2O$ 0.15 M NaH_2PO_2 0.04 M $Na_2MoO_4·2H_2O$ 0.3 M sodium citrate	N_2	1.41@100	[12]
NiMn-LDH/CFC	1 M KOH 0.5 M urea	1.5 mmol $Ni(NO_3)_2·6H_2O$ 0.5 mmol $MnCl_2$ 2.5 mmol HMT	N_2	1.351V@20	[13]
Ni_3Co_1/C-N/CNT (35%)	1 M NaOH 1 M EtOH	$(NH_4)_2S_2O_8$ $Co(CH_3COO)_2·4H_2O$ $Ni(CH_3COO)_2·4H_2O$ (nickel and cobalt molar ratio of 3:1)	CH_3COOH	1.38V@181	[14]
CoNi	1 M KOH 0.33 M glycerol	0.75 M $(NH_4)_2SO_4$ $CoSO_4$ $NiSO_4$	dihydroxyacetone hydroxy pyruvate	~1.3V@10	[15]
Ni_2P-UNMs/NF	1 M KOH 0.125 M benzylamine	5 mL 1 M $NiCl_2$ + 0.5 M $K_2Ni(CN)_4$ 0.2 g NaH_2PO_2	benzonitrile	1.34@10	[16]
VOOH-Ni	1 M KOH 0.33 M urea	2 mmol NH_4VO_3 1 mL of 1.0 M HCl 0.08 mmol $Ni(NO_3)_2·6H_2O$ 2 mL of $N_2H_4·H_2O$	N_2	1.356V@10	[17]

Table S7. The mass of V of 100 mg VO-N/NF nanocomposite in the process of repeated electrocatalytic oxidation.

	Before the electrocatalysis	The first time	The third time	After five chronoamperometric tests
V/mg	1.19	0.96	0.48	0.17

Table S8. The mass of V in 100 mg VO-N/NF nanocomposite and 100 mg VO/NF.

	0.2-VO-N/NF nanocomposite	0.2-VO/NF nanocomposite
V/mg	1.19	1.21

Synthesis of VO/NF

Primarily, $NaVO_3$ (0.2 mmol) and $NiC_4H_6O_4 \cdot 4H_2O$ (0.1mmol) were dissolved in a breaker at room temperature and then poured into a PTFE liner with a piece of nickel foam in it. Next, put it in an oven for 6 h at 140 ^oC for a hydrothermal process. When the reaction is completed, wait for the steel autoclave to cool to room temperature, and then take out the electrode. Eventually, rinse VO/NF and dry it in the vacuum oven.

Synthesis of N/NF

Dissolve melamine (0.2 mmol) in 40 mL deionized water, and then pour the dissolved solution into the PTFE liner with nickel foam in it. Then, transfer it to a 140 ^oC oven for 6 h of hydrothermal process. After the reaction is completed, wait for the steel autoclave to cool to room temperature, and then take it out. Finally, clean the N/NF and dry it in the vacuum oven.

References

1 Y. M. Cao, D. B. Zhang, X. G. Kong, F. Z. Zhang and X. D. Lei, *J. Mater. Sci.*, 2021, **56**, 6689-6703.

2 L. Y. Ming, X. Y. Wu, S. S. Wang, W. M. Wu and C. Z. Lu, *Green Chem.*, 2021, **23**, 7825-7830.

3 J. Zheng, X. L. Chen, X. Zhong, S. Q. Li, T. Z. Liu, G. L. Zhuang, X. N. Li, S. W. Deng, D. H. Mei and J. G. Wang, *Adv. Funct. Mater.*, 2017, **27**, 1704169.

4 H. L. Huang, C. Yu, X. T. Han, H. W. Huang, Q. B. Wei, W. Guo, Z. Wang and J. S. Qiu, *Energy Environ. Sci.*, 2020, **13**, 4990-4999.

5 J. Wan, X. Mu, Y. Jin, J. K. Zhu, Y. C. Xiong, T. Y. Li and R. Li, *Green Chem.*, 2022, **24**, 4870-4876.

6 Y. J. Song, M. W. Yuan, W. L. Su, D. H. Guo, X. B. Chen, G. B. Sun and W. K. Zhang, *Inorg. Chem.*, 2022, **61**, 7308-7317.

7 G. Q. Liu, C. J. Zhao, G. Z. Wang, Y. X. Zhang and H. M. Zhang, *J. Colloid Interface Sci.*, 2018, **532**, 37-46.

8 J. Zhong, Y. L. Shen, P. Zhu, S. Yao and C. H. An, *Nano Res.*, 2023, **16**, 202-208.

9 R. C. Li, P. Y. Kuang, L. X. Wang, H. L. Tang and J. G. Yu, *Chem. Eng. J.*, 2022, **431**, 134137.

10 F. Arshad, T. ul Haq, A. Khan, Y. Haik, I. Hussain and F. Sher, *Energy Convers. Manage.*, 2022, **254**, 115262.

11 Q. Q. Wang, Y. D. Li and C. J. Zhang, *J. Electrochem. Soc.*, 2021, **168**, 076502.

12 H. Jiang, M. Z. Sun, S. L. Wu, B. L. Huang, C. S. Lee and W. J. Zhang, *Adv. Funct. Mater.*, 2021, **31**, 2104951.

13 G. Q. Liu, C. Huang, Z. H. Yang, J. H. Su and W. X. Zhang, *Appl. Catal., A*, 2021, **614**, 118049.

14 Z. L. Deng, Q. F. Yi, Y. Y. Zhang and H. D. Nie, *J. Electroanal. Chem.*, 2017, **803**, 95-103.

15 M. R. Rizk, M. G. Abd El-Moghny, H. H. Abdelhady, W. M. Ragheb, A. H. Mohamed, H. F. Fouad, M. Mohsen, A. S. Kamel and M. S. El-Deab, *Int. J. Hydrogen Energy*, 2022, **47**, 32145-32157.

16 Y. Ding, B. Q. Miao, S. N. Li, Y. C. Jiang, Y. Y. Liu, H. C. Yao and Y. Chen, *Appl. Catal., B*, 2020, **268**, 118393.

17 D. D. Wei, W. J. Tang, N. N. Ma and Y. L. Wang, *Mater. Lett.*, 2021, **291**, 129593.